

The TeraZ Mirage: New Physics Lost in Blind Directions

Mikael Chala* and Juan Carlos Criado†

Departamento de Física Teórica y del Cosmos, Universidad de Granada,
Campus de Fuentenueva, E-18071 Granada, Spain

Michael Spannowsky‡

Institute for Particle Physics Phenomenology,
Department of Physics, Durham University,
Durham DH1 3LE, U.K.

The next generation of high-luminosity electron-positron colliders, such as FCC-ee and CEPC operating at the Z pole (TeraZ), is expected to deliver unprecedented precision in electroweak measurements. These precision observables are typically interpreted within the Standard Model Effective Field Theory (SMEFT), offering a powerful tool to constrain new physics. However, the large number of independent SMEFT operators allows for the possibility of blind directions, parameter combinations to which electroweak precision data are largely insensitive. In this work, we demonstrate that such blind directions are not merely an artefact of agnostic effective field theory scans, but arise generically in realistic ultraviolet completions involving multiple heavy fields. We identify several concrete multi-field extensions of the Standard Model whose low-energy SMEFT projections align with known blind subspaces, and show that these persist even after accounting for renormalisation group evolution and finite one-loop matching effects. Our analysis highlights that the apparent sensitivity to new physics of TeraZ may be significantly overestimated, and that indirect searches alone are often insufficient to rule out broad classes of ultraviolet physics. Complementary high-energy collider probes are therefore essential to fully explore the SMEFT parameter space.

I. INTRODUCTION

The next generation of circular electron-positron colliders, such as the proposed Future Circular Collider (FCC-ee) and the Circular Electron-Positron Collider (CEPC), have the capability to operate at the Z -boson threshold, producing an unprecedented number of Z bosons. This high-statistics environment enables precise measurements of electroweak precision observables (EWPOs), allowing the test of the Standard Model (SM) with high sensitivity. Due to the high luminosity of these experiments, TeraZ, referring to the production of approximately 10^9 Z bosons, offers a window into potential deviations from the SM, thereby serving as a crucial indirect probe of new physics.

Recent studies have highlighted the power of EWPO measurements in setting stringent and model-independent constraints on physics beyond the SM (BSM) [1–3]. It is argued that the precision nature of these observables makes them an essential tool in the search for new physics, as any deviation from SM predictions could signal the presence of new interactions or particles. Historically, a scientific outcome of the Large Electron-Positron Collider (LEP) was that such measurements provide sensitive probes to *some* BSM physics scenarios, guiding theoretical developments and placing constraints on new physics models¹.

Nowadays, the standard approach to interpreting small deviations from the SM is the framework of Effective Field Theory (EFT), which provides a systematic method for parametrising BSM effects in a model-independent manner. The power of indirect searches has been well established in flavour physics, where the Low-Energy Effective Field Theory (LEFT) framework has been instrumental in placing strong constraints on BSM scenarios [5–7]. However, when moving to the SMEFT, the complexity of the problem increases significantly. Unlike LEFT, which operates at lower energies with a relatively small operator basis, SMEFT introduces a vastly larger operator basis, comprising 2,499 independent dimension-six operators [8], many of which contribute to the 26 measured EWPOs. Moreover, this high-dimensional parameter space introduces the possibility of cancellations, where multiple SMEFT operators can conspire to mask new physics contributions, leading to potential blind spots in indirect searches.²

Given the many model parameters and limited physical observables, a key question arises: *Could new physics be*

measured EWPOs to new physics is the scenario of a sequential fourth generation of fermions. In this case, the presence of fourth-generation fermions with masses of a few hundred GeV — i.e., not far above the electron-positron collision energy — could not be excluded due to a blind (or insensitive) direction in the S – T parameter plane [4]. Thus, only Higgs boson measurements excluded a fourth generation at the LHC.

² High-energy hadron colliders possess the advantage to be able to break such blind directions by exploiting different kinematic regions of the phase space, where the operators with non-trivial energy dependence contribute over proportionally compared to the SM, therefore being constrained more tightly [9–13].

* mikael.chala@ugr.es

† jccriadoalamo@ugr.es

‡ michael.spannowsky@durham.ac.uk

¹ A well-known counterexample to the claimed sensitivity of LEP-

just around the corner yet remain undetectable at TeraZ due to such operator cancellations or blind directions?

Addressing this question requires a deeper understanding of how concrete ultraviolet (UV) models project onto the SMEFT parameter space. To our knowledge, previous work has not addressed this question comprehensively. While it was acknowledged that a completely agnostic variation of EFT operator contributions to EWPOs leads to a plethora of blind directions [2], how pronounced they are in more realistic UV models has received little attention. Often, only a single field was integrated out, resulting in a small set of highly correlated EFT operators contributing to the EWPOs in the absence of blind directions [1–3, 14]. Consequently, testing only such scenarios overestimates the prowess of the TeraZ programme on new physics, as realistic UV models generically require the introduction of many new degrees of freedom. In particular, multi-field extensions of the SM may exhibit specific correlations among SMEFT coefficients that could lead to a “nightmare scenario” where new physics resides at energy scales not far away from HL-LHC energy ranges yet invisible to TeraZ. In this work, we make a first investigation of these correlations by exploring simple extensions of the SM and assessing whether they can evade detection at TeraZ. By doing so, we aim to quantify the extent to which TeraZ measurements can generically constrain new physics and to evaluate whether indirect detection remains a robust avenue for probing BSM physics.

A fully comprehensive and exhaustive treatment of all technical aspects is beyond the scope of this work. We introduce controlled simplifications in specific technical steps to maintain clarity in our argument. However, it is crucial to emphasise that relaxing any of these assumptions would only exacerbate the problem of blind directions in EWPO constraints. First, in our analysis, we refrain from marginalising over all effective operators. While such an approach would further expand the region of blind directions, it could also obscure the underlying correlations that relate these blind spots to the dynamics of UV model realisations. Second, we restrict to the sub-sector of the SMEFT spanned by four-fermion interactions with only third-family couplings, and we avoid blind directions that involve unreasonably different sizes of Wilson coefficients (WCs).

In Section II, we display the resulting blind directions of the so-called bottom-up approach, i.e. agnostically varying EFT operators contributing to the EWPOs. Then, in Section III, we consider which UV completions of the SMEFT generate the different blind directions upon integrating the new heavy fields out at tree level. In Section IV, we discuss the fit of selected scenarios to EWPO, including one-loop matching corrections. We offer a summary and conclusions in Section V.

II. EFFECTIVE FIELD THEORY FIT: BOTTOM UP

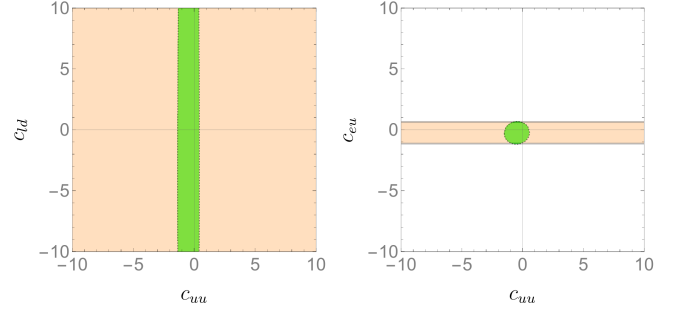


FIG. 1. Examples of EWPO bounds at 3σ on four-fermion regions involving c_{uu} . The orange area enclosed by a solid line includes leading-log RGEs, while we integrate RGEs numerically in the green area enclosed by the dashed line.

In this section, we adopt a bottom-up EFT approach to explore potential blind directions in EWPOs, assuming minimal prior knowledge about the UV origin of the effective operators. We also assess the impact of renormalisation group evolution (RGE), incorporating leading-log RGEs and full numerical integration of the one-loop SMEFT RGEs [15–17].

We consider a total of 26 EWPOs:

$$\text{EWPO} = \left\{ \Gamma_W, \Gamma_W^{e\nu, \mu\nu, \tau\nu}, \Gamma_W^{\text{had}}, \sigma_{\text{had}}, \Gamma_Z, A_{\text{FB}}^{e, \mu, \tau}, A_{\text{FB}}^{s, c, b}, A_{e, \mu, \tau}, A_{s, c, b}, R_{e, \mu, \tau}, R_{s, c, b}, \alpha \right\}, \quad (1)$$

which represent the total decay width of the W , the partial width of the W into different leptons, the partial width of the W into quarks, the total Z hadronic cross section, the Z total decay rate, the forward-backward and left-right asymmetries as well as the ratios of the Z decays into different quarks and leptons and the fine-structure constant. The definitions of these parameters and experimental values can be found in Refs. [18–24]. We take the Fermi constant G_F and the W mass m_W as input parameters.

When restricting to CP-conserving, baryon-number-preserving operators in the Warsaw basis [8] and neglecting flavour structure, we find $\mathcal{O}(50)$ operators, of which 10 independent operators can contribute to EWPOs at tree level [25]. Including RGE evolution, the number of operators contributing to EWPOs grows to 31, out of which 25 can arise from integrating out heavy fields at tree level in realistic UV completions of the SM. While it seems that the 26 EWPOs could overconstrain such a system, not all operators contribute to all EWPOs, and, thus, even imposing such strong constraints on the operators, one finds rather unconstrained subspaces of operators that lead to blind directions. For the numerical results of the fits, we use current constraints on the

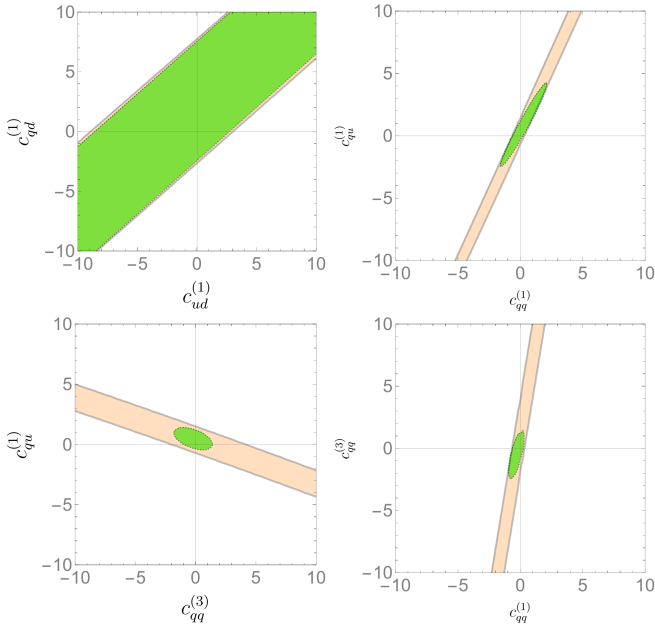


FIG. 2. Regions in the space of $c_{ud}^{(1)}$, $c_{qd}^{(1)}$, $c_{qq}^{(1)}$, $c_{qu}^{(1)}$ and $c_{qq}^{(3)}$ excluded by EWPOs at 3σ . The orange region enclosed by the solid line includes only leading-log RGE effects, while we numerically integrate the RGEs to obtain the green one enclosed by the dashed line.

EWPOs, as implemented in `smelli` [26, 27], rather than relying on any TeraZ projection for their final uncertainties. While such a projection can have a significant effect on the size of the unconstrained region, it will not affect the existence of a blind direction.

We focus on the space spanned by four-fermion operators,³ as they are ubiquitous in models of new physics, arise easily at tree level in UV completions of the SMEFT and, with the exception of \mathcal{O}_{ll} with first family leptons, none enters into EWPO at tree level [25]. The most unconstrained four-fermions involve third-family fermions only, in which we concentrate. Theoretically, one can motivate that new physics couples mostly to the third generation [29–32]. We also ignore $c_{quqd}^{(1)}$, $c_{quqd}^{(8)}$, c_{ledq} , $c_{legu}^{(1)}$ and $c_{legu}^{(3)}$, as they are in general flavour-violating. We follow the notation of Ref. [8] for SMEFT WCs.

We assume WCs to be defined at a scale $\Lambda = 1$ TeV, and study their impact on EWPO at the scale $\sim m_Z$ using the leading-log dimension-six SMEFT RGEs, as well as upon integrating numerically these RGEs. To this latter goal, we rely on `smelli` which is further based on `flavio` [33] and `Wilson` [34].

³ Note that blind directions within the rest of the SMEFT include the obvious cases of \mathcal{O}_ϕ —which affects only the Higgs potential [28]—, $\mathcal{O}_{\phi\square}$ —which enters weakly via RGEs— as well as certain operators that arise only at loop level. Note also that the combination $c_{\phi q}^{(1)} - c_{\phi q}^{(3)}$ is untestable with EWPO but only if it holds right at the Z pole; RGE removes this one.

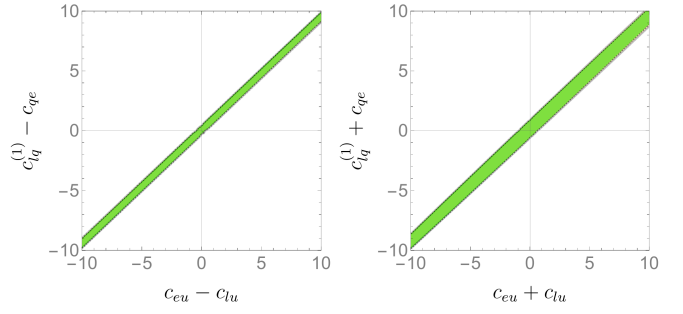


FIG. 3. Regions in the space of c_{ue} , c_{lu} , c_{qe} and $c_{lq}^{(1)}$ excluded by EWPO at 3σ . The orange region enclosed by the solid line includes only leading-log RGE effects, while we numerically integrate the RGEs to obtain the green one enclosed by the dashed line.

To start with, the following WCs do not contribute to EWPO or their contribution is negligible: c_{uu} , c_{dd} , $c_{qu}^{(8)}$, $c_{qd}^{(8)}$, $c_{ud}^{(8)}$, c_{le} , c_{ll} , c_{ed} , c_{ld} . This explains why most of these WCs do not appear in Fig. 1 of Ref. [2]. Out of these, though, c_{uu} is known to be well constrained by two-loop effects captured by RGE re-summation [2, 35–37]; see Fig. 1.

On top of this, we explore all sub-spaces spanned by pairs of the Warsaw-basis four-fermion operators in the search for blind directions. Assuming no disparate sizes for ratios of WCs, we find blind directions in the sub-spaces spanned by $\{c_{qd}^{(1)}, c_{ud}^{(1)}\}$, $\{c_{qq}^{(1)}, c_{qu}^{(1)}\}$, $\{c_{qq}^{(3)}, c_{qu}^{(1)}\}$ and $\{c_{qq}^{(1)}, c_{qq}^{(3)}\}$. However, the last three are gone when RGE resummation is considered;⁴ see Fig. 2. For the one that survives, we have, in TeV:

$$\begin{pmatrix} \Gamma_Z \\ A_b \\ R_{e,\mu,\tau} \end{pmatrix} \sim \begin{pmatrix} -0.0009 & 0.0008 \\ -0.004 & 0.004 \\ -0.01 & 0.009 \end{pmatrix} \begin{pmatrix} c_{ud}^{(1)} \\ c_{qd}^{(1)} \end{pmatrix}, \quad (2)$$

where we have included the most constraining EWPOs on these WCs. The null vector of the corresponding matrix, which describes the blind direction in this sub-space, is given by: $c_{ud}^{(1)} \sim c_{qd}^{(1)}$. It extends to the full set of EWPOs.

There are no blind directions involving three four-fermions (assuming no disparate coefficients as well as survival under RGE resummation). With four, however, we find $c_{eu} \sim c_{qe} \sim c_{lu} \sim c_{lq}^{(1)}$ as well as $c_{eu} \sim c_{qe} \sim -c_{lu} \sim -c_{lq}^{(1)}$; see Fig. 3. Indeed, we have, in TeV:

$$\begin{pmatrix} A_\tau \\ R_\tau \end{pmatrix} \sim \begin{pmatrix} -0.01 & 0.01 & -0.01 & 0.01 \\ -0.19 & -0.24 & 0.23 & 0.20 \end{pmatrix} \begin{pmatrix} c_{eu} \\ c_{lq}^{(1)} \\ c_{lu} \\ c_{qe} \end{pmatrix}. \quad (3)$$

⁴ Approximate flat directions appear also in the planes of $\{c_{eu}, c_{qe}\}$ and $\{c_{lu}, c_{lq}^{(1)}\}$, but here we focus on most robust ones involving all them.

Field	Effective Lagrangian
Ξ_1 $(1, 3)_1$	$+\frac{ y_{\Xi_1} ^2}{M_{\Xi_1}^2} \mathcal{O}_{ll}$
φ $(1, 2)_{1/2}$	$-\frac{ y_{\varphi}^e ^2}{2M_{\varphi}^2} \mathcal{O}_{le} - \frac{ y_{\varphi}^d ^2}{6M_{\varphi}^2} \left(\mathcal{O}_{qd}^{(1)} + 6\mathcal{O}_{qd}^{(8)} \right)$
ω_1 $(3, 1)_{-1/3}$	$+\frac{ y_{\omega_1}^{du} ^2}{3M_{\omega_1}^2} \left(\mathcal{O}_{ud}^{(1)} - 3\mathcal{O}_{ud}^{(8)} \right) + \frac{ y_{\omega_1}^{eu} ^2}{2M_{\omega_1}^2} \mathcal{O}_{eu}$ $+\frac{ y_{\omega_1}^{gl} ^2}{4M_{\omega_1}^2} \left(\mathcal{O}_{lq}^{(1)} - \mathcal{O}_{lq}^{(3)} \right)$
ω_2 $(3, 1)_{2/3}$	$+\frac{ y_{\omega_2} ^2}{M_{\omega_2}^2} \mathcal{O}_{dd}$
ω_4 $(3, 1)_{-4/3}$	$+\frac{ y_{\omega_4}^{ed} ^2}{2M_{\omega_4}^2} \mathcal{O}_{ed}$
Π_1 $(3, 2)_{1/6}$	$-\frac{ y_{\Pi_1} ^2}{2M_{\Pi_1}^2} \mathcal{O}_{ld}$
Π_7 $(3, 2)_{7/6}$	$-\frac{ y_{\Pi_7}^{eq} ^2}{2M_{\Pi_7}^2} \mathcal{O}_{qe} - \frac{ y_{\Pi_7}^{lu} ^2}{2M_{\Pi_7}^2} \mathcal{O}_{lu}$
ζ $(3, 3)_{-1/3}$	$+\frac{ y_{\zeta}^{ql} ^2}{4M_{\zeta}^2} \left(3\mathcal{O}_{lq}^{(1)} + \mathcal{O}_{lq}^{(3)} \right)$
Ω_1 $(6, 1)_{1/3}$	$+\frac{ y_{\Omega_1}^{ud} ^2}{6M_{\Omega_1}^2} \left(2\mathcal{O}_{ud}^{(1)} + 3\mathcal{O}_{ud}^{(8)} \right)$
Ω_2 $(6, 1)_{-2/3}$	$+\frac{ y_{\Omega_2} ^2}{2M_{\Omega_2}^2} \mathcal{O}_{dd}$
Φ $(8, 2)_{1/2}$	$-\frac{ y_{\Phi}^{dq} ^2}{18M_{\Phi}^2} \left(4\mathcal{O}_{qd}^{(1)} - 3\mathcal{O}_{qd}^{(8)} \right)$

Field	Effective Lagrangian
\mathcal{B} $(1, 1)_0$	$-\frac{ g_{\mathcal{B}}^d ^2}{2M_{\mathcal{B}}^2} \mathcal{O}_{dd} - \frac{ g_{\mathcal{B}}^l ^2}{2M_{\mathcal{B}}^2} \mathcal{O}_{ll}$
\mathcal{B}_1 $(1, 1)_1$	$-\frac{ g_{\mathcal{B}_1}^{du} ^2}{3M_{\mathcal{B}_1}^2} \left(\mathcal{O}_{ud}^{(1)} + 6\mathcal{O}_{ud}^{(8)} \right)$
\mathcal{W} $(1, 3)_0$	$-\frac{ g_{\mathcal{W}}^l ^2}{8M_{\mathcal{W}}^2} \mathcal{O}_{ll}$
\mathcal{G} $(8, 1)_0$	$-\frac{ g_{\mathcal{G}}^d ^2}{4M_{\mathcal{G}}^2} \mathcal{O}_{dd}$
\mathcal{G}_1 $(8, 1)_1$	$-\frac{ g_{\mathcal{G}_1} ^2}{9M_{\mathcal{G}_1}^2} \left(4\mathcal{O}_{ud}^{(1)} - 3\mathcal{O}_{ud}^{(8)} \right)$
\mathcal{L}_3 $(1, 2)_{-3/2}$	$+\frac{ g_{\mathcal{L}_3} ^2}{M_{\mathcal{L}_3}^2} \mathcal{O}_{le}$
\mathcal{U}_2 $(3, 1)_{2/3}$	$-\frac{ g_{\mathcal{U}_2}^{ed} ^2}{M_{\mathcal{U}_2}^2} \mathcal{O}_{ed} - \frac{ g_{\mathcal{U}_2}^{lq} ^2}{2M_{\mathcal{U}_2}^2} \left(\mathcal{O}_{lq}^{(1)} + \mathcal{O}_{lq}^{(3)} \right)$
\mathcal{U}_5 $(3, 1)_{5/3}$	$-\frac{ g_{\mathcal{U}_5} ^2}{M_{\mathcal{U}_5}^2} \mathcal{O}_{eu}$
\mathcal{Q}_1 $(3, 2)_{1/6}$	$+\frac{2 g_{\mathcal{Q}_1}^{dq} ^2}{3M_{\mathcal{Q}_1}^2} \left(\mathcal{O}_{qd}^{(1)} - 3\mathcal{O}_{qd}^{(8)} \right) + \frac{ g_{\mathcal{Q}_1}^{ul} ^2}{M_{\mathcal{Q}_1}^2} \mathcal{O}_{lu}$
\mathcal{Q}_5 $(3, 2)_{-5/6}$	$+\frac{ g_{\mathcal{Q}_5}^{dl} ^2}{M_{\mathcal{Q}_5}^2} \mathcal{O}_{ld} + \frac{ g_{\mathcal{Q}_5}^{eq} ^2}{M_{\mathcal{Q}_5}^2} \mathcal{O}_{qe}$
\mathcal{X} $(3, 3)_{2/3}$	$-\frac{ g_{\mathcal{X}} ^2}{8M_{\mathcal{X}}^2} \left(3\mathcal{O}_{lq}^{(1)} - \mathcal{O}_{lq}^{(3)} \right)$
\mathcal{Y}_1 $(\bar{6}, 2)_{1/6}$	$+\frac{ g_{\mathcal{Y}_1} ^2}{3M_{\mathcal{Y}_1}^2} \left(2\mathcal{O}_{qd}^{(1)} + 3\mathcal{O}_{qd}^{(8)} \right)$

TABLE I. *Tree-level matching contributions to potential blind directions from scalars (left) and vectors (right). It is assumed that there is only one non-vanishing coupling to the SM per heavy field, so only one of the terms shown in the expression for the effective Lagrangian generated by each field is present at the same time.*

We refrain from considering larger combinations of WCs for the sake of clarity and tractability. Moreover, as demonstrated in the following section, the class of UV completions that naturally populate the blind subspaces identified above is sufficiently broad to substantiate our main conclusions.

Altogether, we focus on the following combinations of four-fermion operators:

$$\begin{aligned} & \{\mathcal{O}_{dd}, \mathcal{O}_{qu}^{(8)}, \mathcal{O}_{qd}^{(8)}, \mathcal{O}_{ud}^{(8)}, \mathcal{O}_{le}, \mathcal{O}_{ll}, \mathcal{O}_{ed}, \mathcal{O}_{ld}, \\ & \mathcal{O}_{ud}^{(1)} + \mathcal{O}_{qd}^{(1)}, \\ & \mathcal{O}_{eu} + \mathcal{O}_{qe} + \mathcal{O}_{lu} + \mathcal{O}_{lq}^{(1)}, \\ & \mathcal{O}_{eu} + \mathcal{O}_{qe} - \mathcal{O}_{lu} - \mathcal{O}_{lq}^{(1)}\}. \end{aligned} \quad (4)$$

We emphasize that this is not a complete list of all blind directions, but just the simplest ones we have found with the stated assumptions. As we will see in the next section, this is sufficient to illustrate the blindness of TeraZ to some classes of BSM models, since there are several extensions of the SM that generate each of them.

We further observe that finite one-loop SMEFT effects [24] slightly modify, but do not eliminate, the blind directions identified. In the following section, we systematically examine extensions of the SM that, when

matched at tree level onto the SMEFT, give rise to effective operators aligned with these blind subspaces.

III. UV EXTENSIONS OF THE SMEFT

The complete classification of SM extensions that generate dimension-six SMEFT operators at tree level was presented in Ref. [38], building on earlier work [28, 39, 40]. For clarity, we reproduce in Table II only the subset relevant to our analysis, along with the corresponding effective operators they induce. We adopt the coupling notation used in Ref. [38], and note that when multiple heavy fields are present, their contributions to the SMEFT Lagrangian simply add at leading order.

We assume that each heavy field X has a single coupling to the SM, schematically of the form $X\psi_1\psi_2$, where ψ_1 and ψ_2 are SM fermions. The contribution of such a field X to the SMEFT Lagrangian at tree level and dimension six is a linear combination of one or two Warsaw-basis operators with the field content $(\psi_1)^2(\psi_2)^2$. The only pairs of operators that may be generated are $\{\mathcal{O}_x^{(1)}, \mathcal{O}_x^{(8)}\}$, with $x = qu, qd$ and ud . The effects of the $\mathcal{O}_x^{(8)}$ operators on EWPO are all negligible. Thus, each heavy field we consider effectively generates

Blind direction	Extensions			
\mathcal{O}_{ll}	$\{\Xi_1\}$	$\{\mathcal{B}\}$	$\{\mathcal{W}\}$	
\mathcal{O}_{le}	$\{\varphi\}$	$\{\mathcal{L}_3\}$		
\mathcal{O}_{dd}	$\{\omega_2\}$	$\{\Omega_2\}$	$\{\mathcal{G}\}$	
\mathcal{O}_{ed}	$\{\omega_4\}$	$\{\mathcal{U}_2\}$		
\mathcal{O}_{ld}	$\{\Pi_1\}$	$\{\mathcal{L}_3\}$		
$\mathcal{O}_{ud}^{(1)} + \mathcal{O}_{qd}^{(1)}$	$\{\varphi, \mathcal{B}_1\}$ $\{\Omega_1, \mathcal{Q}_1\}$	$\{\varphi, \mathcal{G}_1\}$ $\{\Omega_1, \mathcal{Y}_1\}$	$\{\omega_1, \mathcal{Q}_1\}$ $\{\Phi, \mathcal{B}_1\}$	$\{\omega_1, \mathcal{Y}_1\}$ $\{\Phi, \mathcal{G}_1\}$
$\mathcal{O}_{eu} + \mathcal{O}_{qe}$ + $\mathcal{O}_{lu} + \mathcal{O}_{lq}^{(1)}$	$\{\omega_1, \mathcal{Q}_5, \mathcal{Q}_1, \omega_1, \zeta\}$ $\{\mathcal{U}_5, \Pi_7, \Pi_7, \omega_1, \mathcal{X}\}$	$\{\omega_1, \mathcal{Q}_5, \mathcal{Q}_1, \zeta, \mathcal{U}_2\}$ $\{\mathcal{U}_5, \Pi_7, \Pi_7, \mathcal{U}_2, \mathcal{X}\}$		
$\mathcal{O}_{eu} + \mathcal{O}_{qe}$ - $\mathcal{O}_{lu} - \mathcal{O}_{lq}^{(1)}$	$\{\omega_1, \mathcal{Q}_5, \Pi_7, \omega_1, \mathcal{X}\}$ $\{\mathcal{U}_5, \Pi_7, \mathcal{Q}_1, \omega_1, \zeta\}$	$\{\omega_1, \mathcal{Q}_5, \Pi_7, \mathcal{U}_2, \mathcal{X}\}$ $\{\mathcal{U}_5, \Pi_7, \mathcal{Q}_1, \zeta, \mathcal{U}_2\}$		

TABLE II. *Extensions of the SM that generate blind directions.*

a single operator relevant for EWPO.

Our aim is to identify which tree-level completions of the SMEFT, involving a limited number of heavy fields, give rise to effective interactions aligned with the blind subspace defined in Eq. (4). We make use of MatchingDB [41] for this purpose.

We start with the following single-field extensions that generate only an unconstrained operator:

- Ξ_1 , \mathcal{B} and \mathcal{W} generate \mathcal{O}_{ll} .
- φ and \mathcal{L}_3 generate \mathcal{O}_{le} .
- ω_2 , Ω_2 , \mathcal{B} and \mathcal{G} generate \mathcal{O}_{dd} .
- ω_4 and \mathcal{U}_2 generate \mathcal{O}_{ed} .
- Π_1 and \mathcal{L}_3 generate \mathcal{O}_{ld} .

The blind direction $c_{ud}^{(1)} \simeq c_{qd}^{(1)}$ can not be generated by single-field extensions; at least two fields are needed, and it can be read from Table II. It involves φ or Φ with either \mathcal{B}_1 or \mathcal{G}_1 as well as ω_1 or Ω_1 with either \mathcal{Q}_1 or \mathcal{Y}_1 .

Concerning $c_{eu} \sim c_{qe} \sim \pm c_{lu} \sim \pm c_{lq}^{(1)}$, there are eight five-field extensions that generate this blind direction. They are given by any combination of a pair of fields from the list

$$\{(\omega_1, \mathcal{Q}_5), (\mathcal{U}_5, \Pi_7)\} \quad (5)$$

with a triad of fields from the list

$$\{(\Pi_7, \omega_1, \mathcal{X}), (\Pi_7, \mathcal{U}_2, \mathcal{X}), (\mathcal{Q}_1, \omega_1, \zeta), (\mathcal{Q}_1, \zeta, \mathcal{U}_2)\}. \quad (6)$$

If any of the fields is repeated in the combination, it is understood that two copies of that field are present, each with different couplings to the SM. All these possible combinations are displayed in Table III.

One might expect that finite one-loop matching effects, those not already captured by renormalisation group evolution, could lift the blind directions. However, we have verified explicitly that this is not the case for the

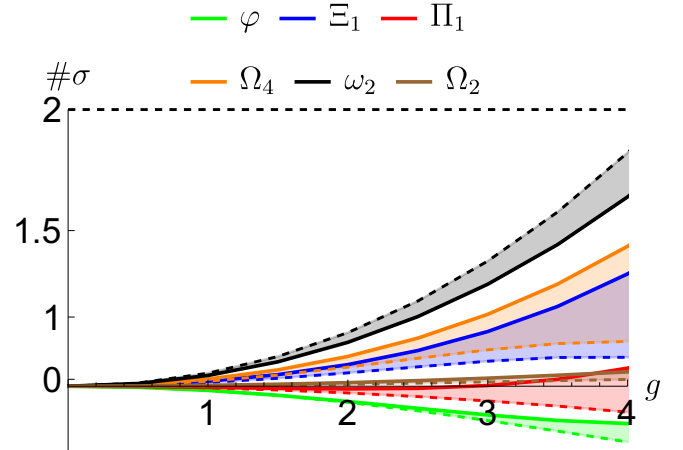


FIG. 4. *Sensitivity of EWPO to different single-scalar extensions of the SMEFT as a function of their only coupling to the SM. The solid (dash) line includes tree-level and leading-log RGE (RGE resummation and finite one-loop matching corrections).*

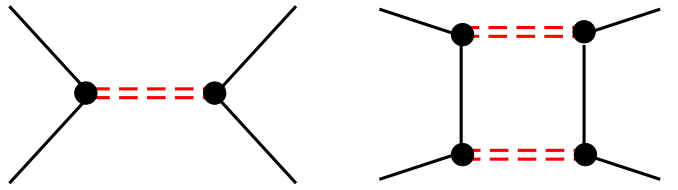


FIG. 5. *Tree-level and one-loop diagrams contributing to four-fermion interactions.*

single-scalar extensions; see Fig. 4. To this end, we performed one-loop matching onto the SMEFT using dedicated routines, with the assistance of **SOLD** [42, 43] and **matchmakereft** [44]. We note that integrating out massive vector fields at one loop is non-trivial without a complete description of the underlying spontaneously broken theory, and is currently not supported by existing automated tools [42–45]. For brevity and cohesion, we omit the technical details of the matching procedure.

The limited impact of finite one-loop matching corrections on lifting blind directions can be attributed to the fact that, in the limit of vanishing SM couplings, these corrections predominantly generate operators that lie within the same blind subspace defined in Eq. (4). For instance, the scalar field Π_1 induces finite one-loop contributions to \mathcal{O}_{ll} and \mathcal{O}_{dd} , in addition to the tree-level contribution to \mathcal{O}_{ld} , via diagrams such as those shown in Fig. 5.

For higher-field extensions, we restrict our analysis to the scalar components, which can be consistently integrated out within existing one-loop matching frameworks. In what follows, we present explicit results for three illustrative scenarios.

IV. FIT FOR MULTI-FIELD MODELS

Finally, in this section, we fit three selected UV scenarios to the EWPOs, including the one-loop matching corrections from integrating out the heavy scalars involved.

Example 1

We consider the following UV fields:

- $\omega_1 \sim (3, 1)_{-1/3}$ (a scalar leptoquark),
- $\mathcal{Q}_1 \sim (3, 1)_{1/6}$ (a vector leptoquark).

The appearance of multiple leptoquarks is typical of GUTs and string-inspired models; see e.g. Ref. [46]. They are also common in models explaining flavour anomalies; see e.g. Refs. [47–50].

The UV interaction Lagrangian reads:

$$\mathcal{L}_{UV} = g_{\omega_1}^{ud} \epsilon_{ABC} \omega_1^{A\dagger} \bar{d}_R^B u_R^C + y_{\mathcal{Q}_1}^{dq} \epsilon_{ABC} \mathcal{Q}_1^{A\mu\dagger} \bar{d}_R^B \gamma_\mu i \sigma_2 q_L^C + \text{h.c.} \quad (7)$$

Likewise, the effective Lagrangian is:

$$\mathcal{L}_{\text{eff}} = \frac{|y_{\omega_1}^{du}|^2}{3M_{\omega_1}^2} \left(\mathcal{O}_{ud}^{(1)} - 3\mathcal{O}_{ud}^{(8)} \right) + \frac{2|g_{\mathcal{Q}_1}^{dq}|^2}{3M_{\mathcal{Q}_1}^2} \left(\mathcal{O}_{qd}^{(1)} - 3\mathcal{O}_{qd}^{(8)} \right). \quad (8)$$

This gives rise to the following blind direction:

$$\frac{|y_{\omega_1}^{du}|}{M_{\omega_1}} \simeq \sqrt{2} \frac{|g_{\mathcal{Q}_1}^{dq}|}{M_{\mathcal{Q}_1}}. \quad (9)$$

The bounds imposed by EWPO on the parameter space of this model, obtained again with `smelli`, are shown in Fig. 6. It is apparent that one-loop matching corrections only modify slightly the tree-level blind direction.

Example 2

Next, we consider the following UV fields:

- $\varphi \sim (1, 2)_{1/2}$ (a second Higgs doublet),
- $\mathcal{B}_1 \sim (1, 1)_1$ (a W').

Such a field content may be found in the left-right SUSY model, in which the SM gauge group is embedded into $SU(3)_C \times SU(2)_L \times SU(2)_R \times U(1)_{B-L}$. The W' arises from the spontaneous breaking of $SU(2)_R$, while the second Higgs comes from the decomposition of Higgs bidoublets required by SUSY [51, 52].

The UV interaction Lagrangian reads:

$$\mathcal{L}_{UV} = y_\varphi^d \varphi^\dagger \bar{d}_R q_L + g_{\mathcal{B}_1}^{du} \mathcal{B}_1^\dagger \bar{d}_R \gamma_\mu u_R + \text{h.c.} \quad (10)$$

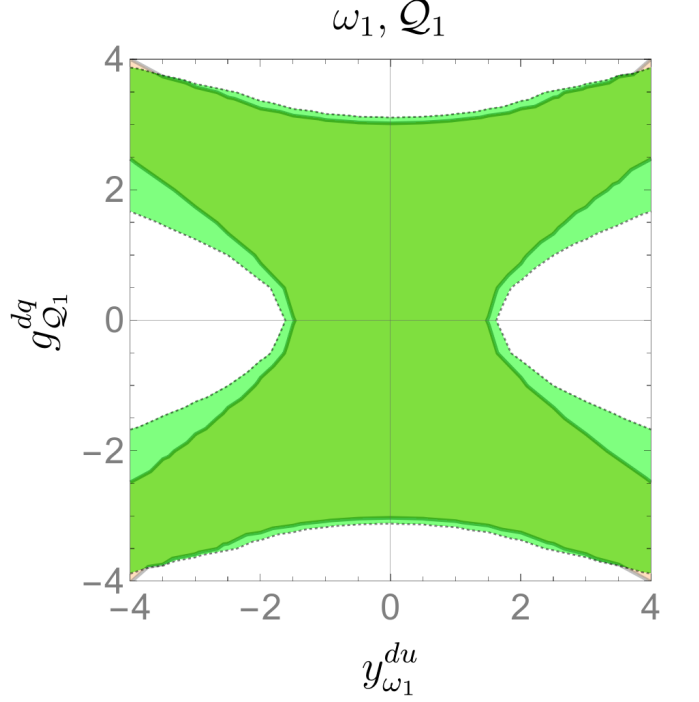


FIG. 6. Region of the parameter space excluded by EWPOs at 1σ including tree-level and leading-log RGes (dark area enclosed by solid line) and including one-loop matching scalar corrections and RGE resummation (light area enclosed by dashed line) for a UV model involving two leptoquarks ω_1 and \mathcal{Q}_1 . The masses of the scalar and the vector are assumed equal and of 1 TeV.

In turn, the effective Lagrangian is:

$$\mathcal{L}_{\text{eff}} = -\frac{|y_\varphi^d|^2}{6M_\varphi^2} \left(\mathcal{O}_{qu}^{(1)} + 6\mathcal{O}_{qu}^{(8)} \right) - \frac{|g_{\mathcal{B}_1}^{du}|^2}{3M_{\mathcal{B}_1}^2} \left(\mathcal{O}_{ud}^{(1)} + 6\mathcal{O}_{ud}^{(8)} \right). \quad (11)$$

This gives rise to the following blind direction:

$$\frac{|y_\varphi^d|}{M_\varphi} \simeq \sqrt{2} \frac{|g_{\mathcal{B}_1}^{du}|}{M_{\mathcal{B}_1}}. \quad (12)$$

Using again `smelli`, we show the space constrained by EWPOs in Fig. 7. Just like before, one-loop matching corrections are negligible.

Example 3

As an example of a UV model that generates the blind direction $c_{eu} \sim c_{qe} \sim -c_{lu} \sim -c_{lq}^{(1)}$, we consider the following field content:

- Scalars: $\omega_1 \sim (3, 1)_{-1/3}$ and $\Pi_7 \sim (3, 2)_{7/6}$,
- Vectors: $\mathcal{U}_2 \sim (3, 1)_{2/3}$, $\mathcal{Q}_5 \sim (3, 2)_{-5/6}$ and $\mathcal{X} \sim (3, 3)_{2/3}$,

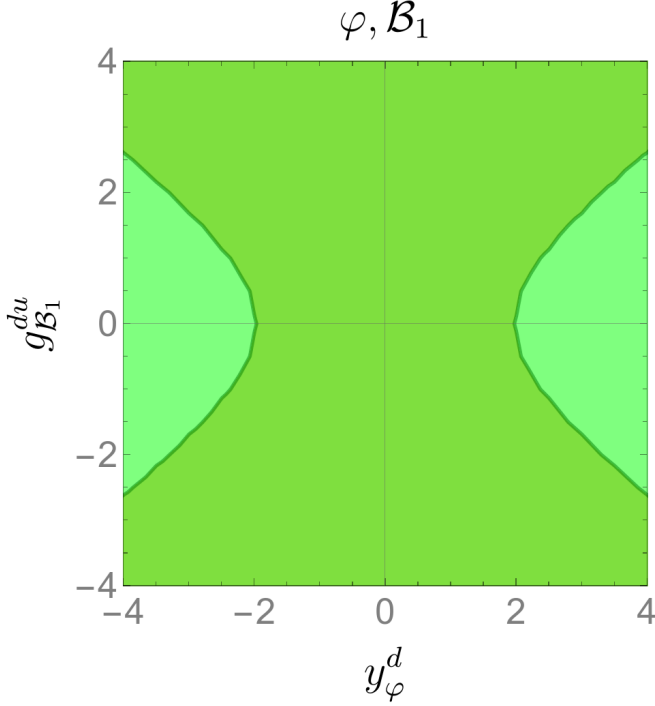


FIG. 7. Same as Fig. 6 but for an UV completion of the SMEFT involving φ and \mathcal{B}_1 .

with interaction Lagrangian

$$\begin{aligned} \mathcal{L}_{\text{UV}} = & y_{\omega_1}^{eu} \omega_1^\dagger \bar{e}_R^c u_R + g_{\mathcal{Q}_5}^{eq} \mathcal{Q}_5^{\mu\dagger} \bar{e}_R^c \gamma_\mu q_L + y_{\Pi_7}^{lu} \Pi_7^\dagger i\sigma_2 \bar{l}_L^T u_R \\ & + g_{\mathcal{U}_2}^{lq} \mathcal{U}_2^{\mu\dagger} \bar{l}_L \gamma_\mu q_L + \frac{g_{\mathcal{X}}}{2} \mathcal{X}^{a\mu\dagger} \bar{l}_L \gamma_\mu \sigma^a q_L + \text{h.c.} \end{aligned} \quad (13)$$

All these heavy fields are leptoquarks, which arise in UV models pointed out in Example 2. Integrating them out gives

$$\begin{aligned} \mathcal{L}_{\text{eff}} = & \frac{|y_{\omega_1}^{eu}|^2}{2M_{\omega_1}^2} \mathcal{O}_{eu} + \frac{|g_{\mathcal{Q}_5}^{eq}|^2}{M_{\mathcal{Q}_5}^2} \mathcal{O}_{eq} - \frac{|y_{\Pi_7}^{lu}|^2}{2M_{\Pi_7}^2} \mathcal{O}_{lu} \\ & - \left(\frac{|g_{\mathcal{U}_2}^{lq}|^2}{2M_{\mathcal{U}_2}^2} + \frac{3|g_{\mathcal{X}}|^2}{8M_{\mathcal{X}}^2} \right) \mathcal{O}_{lq}^{(1)} \\ & - \left(\frac{|g_{\mathcal{U}_2}^{lq}|^2}{2M_{\mathcal{U}_2}^2} - \frac{|g_{\mathcal{X}}|^2}{8M_{\mathcal{X}}^2} \right) \mathcal{O}_{lq}^{(3)}. \end{aligned} \quad (14)$$

The blind direction arises when

$$\frac{|y_{\omega_1}^{eu}|}{M_{\omega_1}} \sim \sqrt{2} \frac{|g_{\mathcal{Q}_5}^{eq}|}{M_{\mathcal{Q}_5}} \sim \frac{|y_{\Pi_7}^{lu}|}{M_{\Pi_7}} \sim 2 \frac{|g_{\mathcal{U}_2}^{lq}|}{M_{\mathcal{U}_2}} \sim \frac{|g_{\mathcal{X}}|}{M_{\mathcal{X}}}. \quad (15)$$

The region of the parameter space constrained by EWPOs is shown in Fig. 8.

V. SUMMARY AND CONCLUSIONS

In this work, we have investigated blind directions in the SMEFT, focusing on the four-fermion sector with

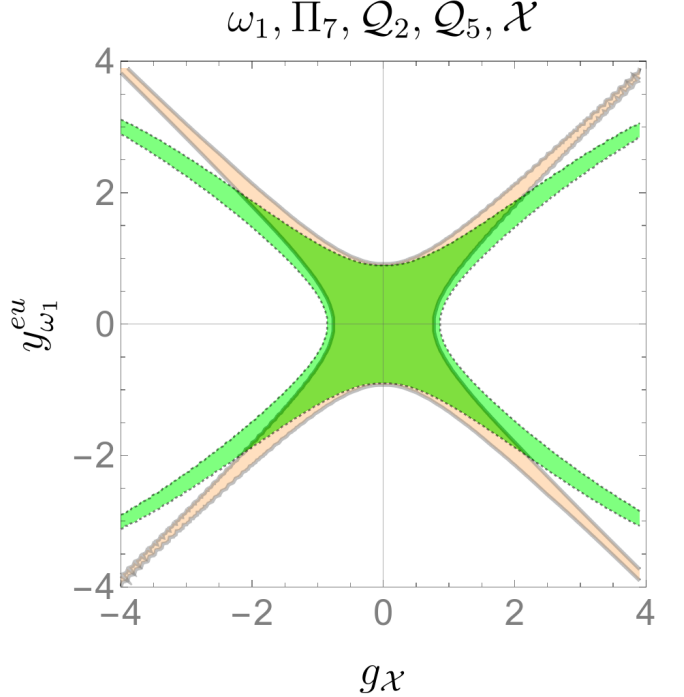


FIG. 8. Same as Fig. 6 but for an UV model with ω_1 , Π_7 , \mathcal{Q}_2 , \mathcal{Q}_5 and \mathcal{X} , assuming $\sqrt{2}g_{\mathcal{Q}_5}^{eq} = 2g_{\mathcal{U}_2}^{lq} = g_{\mathcal{X}}$ and $y_{\Pi_7}^{lu} = y_{\omega_1}^{eu}$.

third-family WCs. By restricting our analysis to this sector, we have identified an 11-dimensional subspace that remains blind to EWPOs, even after accounting for improved perturbation theory. We have shown that simple multi-field UV completions of the SM, where the heavy fields are integrated out at tree level, can reside within this blind subspace. One-loop matching corrections do not alter the persistence of these blind directions.

Our results make it clear that blind directions are not isolated curiosities but rather a systematic and generic feature of realistic SMEFT completions. Even under simplifying assumptions, such as limiting to third-generation couplings, working with tree-level matching, and considering only a modest number of operators, we identify multiple blind directions that evade the entire suite of EWPOs at TeraZ. The situation becomes even more pronounced when considering that 25 independent four-fermion operators (which can all be generated at tree level) are constrained by only 26 EWPOs, many of which are sensitive to overlapping subsets of operators. The apparent over-constrained nature of the system is therefore misleading. This imbalance, together with correlated SMEFT contributions from realistic multi-field UV completions, makes blind directions not just possible but likely. In this sense, our findings reveal that the problem is structural rather than exceptional, and underline the inherent limitations of relying solely on precision measurements, even at the unprecedented luminosities of TeraZ, to comprehensively probe new physics.

These results highlight the need for complementary

high-energy collider experiments that can explore different kinematic regimes and help resolve the degeneracies present in precision electroweak measurements. This need becomes even more pressing as the typical scale of new physics increases beyond the 1 TeV benchmark used in our analysis. We also note that our fits are based on current experimental data rather than projected sensitivities for TeraZ. Nevertheless, our findings are in good agreement with previous studies where comparisons are possible. For example, despite differences in coupling assumptions, Fig. 3 of Ref. [3] shows that several single-field extensions remain unconstrained beyond 2 TeV.

It is also important to emphasize that the problem of blind directions becomes more severe when the simplifying assumptions used in this work are relaxed. Allowing for couplings to additional fermion families or permitting non-trivial hierarchies among WCs would further enlarge the space of blind directions, making it even more challenging to derive robust constraints from precision elec-

troweenk data alone. A comprehensive study of this more general scenario is left for future work.

ACKNOWLEDGMENTS

This work has received funding from MI-CIU/AEI/10.13039/501100011033 and ERDF/EU (grants PID2022-139466NB-C22 and PID2021-128396NB-I00), from the Junta de Andalucía grants FQM 101 and P21-00199 as well as from The Royal Society programmes Newton International Fellowship Alumni follow-on and International Exchanges under grant numbers AL-231018 and IES-R1-221239, respectively. MC and JCC are further supported by the Ramón y Cajal program under grants RYC2019-027155-I and RYC2021-030842-I; respectively.

[1] J. Gargalionis, J. Quevillon, P. N. H. Vuong, and T. You, Linear Standard Model extensions in the SMEFT at one loop and Tera-Z, (2024), [arXiv:2412.01759 \[hep-ph\]](https://arxiv.org/abs/2412.01759).

[2] V. Maura, B. A. Stefanek, and T. You, Accuracy complements energy: electroweak precision tests at Tera-Z, (2024), [arXiv:2412.14241 \[hep-ph\]](https://arxiv.org/abs/2412.14241).

[3] L. Allwicher, M. McCullough, and S. Renner, New physics at Tera-Z: precision renormalised, *JHEP* **02**, 164, [arXiv:2408.03992 \[hep-ph\]](https://arxiv.org/abs/2408.03992).

[4] G. D. Kribs, T. Plehn, M. Spannowsky, and T. M. P. Tait, Four generations and Higgs physics, *Phys. Rev. D* **76**, 075016 (2007), [arXiv:0706.3718 \[hep-ph\]](https://arxiv.org/abs/0706.3718).

[5] G. Buchalla, A. J. Buras, and M. E. Lautenbacher, Weak decays beyond leading logarithms, *Rev. Mod. Phys.* **68**, 1125 (1996), [arXiv:hep-ph/9512380](https://arxiv.org/abs/hep-ph/9512380).

[6] A. J. Buras, P. Gambino, M. Gorbahn, S. Jager, and L. Silvestrini, Universal unitarity triangle and physics beyond the standard model, *Phys. Lett. B* **500**, 161 (2001), [arXiv:hep-ph/0007085](https://arxiv.org/abs/hep-ph/0007085).

[7] D. Buttazzo, A. Greljo, G. Isidori, and D. Marzocca, B-physics anomalies: a guide to combined explanations, *JHEP* **11**, 044, [arXiv:1706.07808 \[hep-ph\]](https://arxiv.org/abs/1706.07808).

[8] B. Grzadkowski, M. Iskrzynski, M. Misiak, and J. Rosiek, Dimension-Six Terms in the Standard Model Lagrangian, *JHEP* **10**, 085, [arXiv:1008.4884 \[hep-ph\]](https://arxiv.org/abs/1008.4884).

[9] C. Englert, R. Kogler, H. Schulz, and M. Spannowsky, Higgs coupling measurements at the LHC, *Eur. Phys. J. C* **76**, 393 (2016), [arXiv:1511.05170 \[hep-ph\]](https://arxiv.org/abs/1511.05170).

[10] C. Englert, R. Kogler, H. Schulz, and M. Spannowsky, Higgs characterisation in the presence of theoretical uncertainties and invisible decays, *Eur. Phys. J. C* **77**, 789 (2017), [arXiv:1708.06355 \[hep-ph\]](https://arxiv.org/abs/1708.06355).

[11] R. Franceschini, G. Panico, A. Pomarol, F. Riva, and A. Wulzer, Electroweak Precision Tests in High-Energy Diboson Processes, *JHEP* **02**, 111, [arXiv:1712.01310 \[hep-ph\]](https://arxiv.org/abs/1712.01310).

[12] S. Banerjee, C. Englert, R. S. Gupta, and M. Spannowsky, Probing Electroweak Precision Physics via boosted Higgs-strahlung at the LHC, *Phys. Rev. D* **98**, 095012 (2018), [arXiv:1807.01796 \[hep-ph\]](https://arxiv.org/abs/1807.01796).

[13] A. Belvedere, C. Englert, R. Kogler, and M. Spannowsky, Dispelling the \sqrt{L} myth for the High-Luminosity LHC, *Eur. Phys. J. C* **84**, 715 (2024), [arXiv:2402.07985 \[hep-ph\]](https://arxiv.org/abs/2402.07985).

[14] S. Das Bakshi, J. Chakrabortty, and M. Spannowsky, Classifying Standard Model Extensions Effectively with Precision Observables, *Phys. Rev. D* **103**, 056019 (2021), [arXiv:2012.03839 \[hep-ph\]](https://arxiv.org/abs/2012.03839).

[15] E. E. Jenkins, A. V. Manohar, and M. Trott, Renormalization Group Evolution of the Standard Model Dimension Six Operators II: Yukawa Dependence, *JHEP* **01**, 035, [arXiv:1310.4838 \[hep-ph\]](https://arxiv.org/abs/1310.4838).

[16] E. E. Jenkins, A. V. Manohar, and M. Trott, Renormalization Group Evolution of the Standard Model Dimension Six Operators I: Formalism and lambda Dependence, *JHEP* **10**, 087, [arXiv:1308.2627 \[hep-ph\]](https://arxiv.org/abs/1308.2627).

[17] R. Alonso, E. E. Jenkins, A. V. Manohar, and M. Trott, Renormalization Group Evolution of the Standard Model Dimension Six Operators III: Gauge Coupling Dependence and Phenomenology, *JHEP* **04**, 159, [arXiv:1312.2014 \[hep-ph\]](https://arxiv.org/abs/1312.2014).

[18] First combination of Tevatron and LHC measurements of the top-quark mass, (2014), [arXiv:1403.4427 \[hep-ex\]](https://arxiv.org/abs/1403.4427).

[19] M. Davier, A. Hoecker, B. Malaescu, and Z. Zhang, Reevaluation of the Hadronic Contributions to the Muon $g-2$ and to $\alpha(MZ)$, *Eur. Phys. J. C* **71**, 1515 (2011), [Erratum: Eur.Phys.J.C 72, 1874 (2012)], [arXiv:1010.4180 \[hep-ph\]](https://arxiv.org/abs/1010.4180).

[20] T. E. W. Group (CDF, D0), 2012 Update of the Combination of CDF and D0 Results for the Mass of the W Boson, (2012), [arXiv:1204.0042 \[hep-ex\]](https://arxiv.org/abs/1204.0042).

[21] S. Schael *et al.* (ALEPH, DELPHI, L3, OPAL, SLD, LEP Electroweak Working Group, SLD Electroweak Group, SLD Heavy Flavour Group), Precision electroweak measurements on the Z resonance, *Phys. Rept.* **427**, 257 (2006), [arXiv:hep-ex/0509008](https://arxiv.org/abs/hep-ex/0509008).

[22] Precision Electroweak Measurements and Constraints on the Standard Model, (2010), [arXiv:1012.2367 \[hep-ex\]](https://arxiv.org/abs/1012.2367).

[23] S. Navas *et al.* (Particle Data Group), Review of particle physics, *Phys. Rev. D* **110**, 030001 (2024).

[24] A. Biekötter and B. D. Pecjak, Analytic results for electroweak precision observables at NLO in SMEFT, (2025), arXiv:2503.07724 [hep-ph].

[25] J. de Blas, M. Chala, and J. Santiago, Renormalization Group Constraints on New Top Interactions from Electroweak Precision Data, *JHEP* **09**, 189, arXiv:1507.00757 [hep-ph].

[26] J. Aebischer, J. Kumar, P. Stangl, and D. M. Straub, A Global Likelihood for Precision Constraints and Flavour Anomalies, *Eur. Phys. J. C* **79**, 509 (2019), arXiv:1810.07698 [hep-ph].

[27] P. Stangl, smelli – the SMEFT Likelihood, *PoS TOOLS2020*, 035 (2021), arXiv:2012.12211 [hep-ph].

[28] J. de Blas, M. Chala, M. Perez-Victoria, and J. Santiago, Observable Effects of General New Scalar Particles, *JHEP* **04**, 078, arXiv:1412.8480 [hep-ph].

[29] R. Contino, Y. Nomura, and A. Pomarol, Higgs as a Holographic Pseudo Goldstone Boson, *Nucl. Phys. B* **671**, 148 (2003), arXiv:hep-ph/0306259.

[30] G. Panico and A. Wulzer, *The Composite Nambu-Goldstone Higgs*, Vol. 913 (Springer, 2016) arXiv:1506.01961 [hep-ph].

[31] J. Davighi and G. Isidori, Non-universal gauge interactions addressing the inescapable link between Higgs and flavour, *JHEP* **07**, 147, arXiv:2303.01520 [hep-ph].

[32] Y. Chung and F. Goertz, Third-generation-philic hidden naturalness, *Phys. Rev. D* **110**, 115019 (2024), arXiv:2311.17169 [hep-ph].

[33] D. M. Straub, flavio: a Python package for flavour and precision phenomenology in the Standard Model and beyond, (2018), arXiv:1810.08132 [hep-ph].

[34] J. Aebischer, J. Kumar, and D. M. Straub, Wilson: a Python package for the running and matching of Wilson coefficients above and below the electroweak scale, *Eur. Phys. J. C* **78**, 1026 (2018), arXiv:1804.05033 [hep-ph].

[35] L. Allwicher, G. Isidori, J. M. Lizana, N. Selimovic, and B. A. Stefanek, Third-family quark-lepton Unification and electroweak precision tests, *JHEP* **05**, 179, arXiv:2302.11584 [hep-ph].

[36] L. Allwicher, C. Cornellà, G. Isidori, and B. A. Stefanek, New physics in the third generation. A comprehensive SMEFT analysis and future prospects, *JHEP* **03**, 049, arXiv:2311.00020 [hep-ph].

[37] B. A. Stefanek, Non-universal probes of composite Higgs models: new bounds and prospects for FCC-ee, *JHEP* **09**, 103, arXiv:2407.09593 [hep-ph].

[38] J. de Blas, J. C. Criado, M. Perez-Victoria, and J. Santiago, Effective description of general extensions of the Standard Model: the complete tree-level dictionary, *JHEP* **03**, 109, arXiv:1711.10391 [hep-ph].

[39] F. del Aguila, M. Perez-Victoria, and J. Santiago, Observable contributions of new exotic quarks to quark mixing, *JHEP* **09**, 011, arXiv:hep-ph/0007316.

[40] F. del Aguila, J. de Blas, and M. Perez-Victoria, Effects of new leptons in Electroweak Precision Data, *Phys. Rev. D* **78**, 013010 (2008), arXiv:0803.4008 [hep-ph].

[41] L. Allwicher *et al.*, Computing tools for effective field theories: SMEFT-Tools 2022 Workshop Report, 14–16th September 2022, Zürich, *Eur. Phys. J. C* **84**, 170 (2024), arXiv:2307.08745 [hep-ph].

[42] G. Guedes, P. Olgoso, and J. Santiago, Towards the one loop IR/UV dictionary in the SMEFT: One loop generated operators from new scalars and fermions, *SciPost Phys.* **15**, 143 (2023), arXiv:2303.16965 [hep-ph].

[43] G. Guedes and P. Olgoso, From the EFT to the UV: the complete SMEFT one-loop dictionary, (2024), arXiv:2412.14253 [hep-ph].

[44] A. Carmona, A. Lazopoulos, P. Olgoso, and J. Santiago, Matchmakereft: automated tree-level and one-loop matching, *SciPost Phys.* **12**, 198 (2022), arXiv:2112.10787 [hep-ph].

[45] J. Fuentes-Martín, M. König, J. Pagès, A. E. Thomsen, and F. Wilsch, A proof of concept for matchete: an automated tool for matching effective theories, *Eur. Phys. J. C* **83**, 662 (2023), arXiv:2212.04510 [hep-ph].

[46] D. Croon, T. E. Gonzalo, L. Graf, N. Košnik, and G. White, GUT Physics in the era of the LHC, *Front. in Phys.* **7**, 76 (2019), arXiv:1903.04977 [hep-ph].

[47] N. Assad, B. Fornal, and B. Grinstein, Baryon Number and Lepton Universality Violation in Leptoquark and Diquark Models, *Phys. Lett. B* **777**, 324 (2018), arXiv:1708.06350 [hep-ph].

[48] G. D’Amico, M. Nardecchia, P. Panci, F. Sannino, A. Strumia, R. Torre, and A. Urbano, Flavour anomalies after the R_{K^*} measurement, *JHEP* **09**, 010, arXiv:1704.05438 [hep-ph].

[49] L. Calibbi, A. Crivellin, and T. Li, Model of vector leptoquarks in view of the B -physics anomalies, *Phys. Rev. D* **98**, 115002 (2018), arXiv:1709.00692 [hep-ph].

[50] C. Cornellà, J. Fuentes-Martin, and G. Isidori, Revisiting the vector leptoquark explanation of the B -physics anomalies, *JHEP* **07**, 168, arXiv:1903.11517 [hep-ph].

[51] F. del Aguila, J. de Blas, and M. Perez-Victoria, Electroweak Limits on General New Vector Bosons, *JHEP* **09**, 033, arXiv:1005.3998 [hep-ph].

[52] M. Hirsch, M. E. Krauss, T. Opferkuch, W. Porod, and F. Staub, A constrained supersymmetric left-right model, *JHEP* **03**, 009, arXiv:1512.00472 [hep-ph].

[53] A. Greljo and B. A. Stefanek, Third family quark-lepton unification at the TeV scale, *Phys. Lett. B* **782**, 131 (2018), arXiv:1802.04274 [hep-ph].